Nonadiabatic geometric phase in a doubly driven two-level system

Weixin Liu(刘伟新)[1], Tao Wang(汪涛)[2,3,†], and Weidong Li(李卫东)[4]

[1] *Institute of Theoretical Physics and Department of Physics, State Key Laboratory of Quantum Optics and Quantum Optics Devices, Collaborative Innovation Center of Extreme Optics, Shanxi University, Taiyuan* 030006, *China*
[2] *Department of Physics, and Center of Quantum Materials and Devices, Chongqing University, Chongqing* 401331, *China*
[3] *Chongqing Key Laboratory for Strongly Coupled Physics, Chongqing* 401331, *China*
[4] *Shenzhen Key Laboratory of Ultraintense Laser and Advanced Material Technology, Center for Advanced Material Diagnostic Technology, and College of Engineering Physics, Shenzhen Technology University, Shenzhen* 518118, *China*

(Received 28 May 2022; revised manuscript received 6 August 2022; accepted manuscript online 16 August 2022)

We study theoretically the nonadiabatic geometric phase of a doubly driven two-level system with an additional relative phase between the two driving modes introduced in. It is shown that the time evolution of the system strongly depends on this relative phase. The condition for the system returning to its initial state after a single period is given by the means of the Landau–Zener–Stückelberg–Majorana destructive interference. The nonadiabatic geometric phase accompanying a cyclic evolution is shown to be related to the Stokes phase as well as this relative phase. By controlling the relative phase, the geometric phase can characterize two distinct phases in the adiabatic limit.

Keywords: two-level system, geometric phase, Landau–Zener–Stückelberg–Majorana interference

PACS: 03.65.Vf, 03.67.Lx, 42.50.Gy **DOI:** 10.1088/1674-1056/ac89e3

1. Introduction

Ever since its discovery by Berry[1] the gauge invariant geometric phase has attracted immense interest both in theoretical and experimental study.[2–13] Originally, Berry pointed out that the quantum system will acquire a nontrivial phase factor in the instantaneous eigenstate of the time-dependent Hamiltonian in addition to the familiar dynamic phase, when slowly, adiabatically changing the Hamiltonian around a circuit in the parameter space. Subsequently, Aharonov and Anandan extended the adiabatic Berry phase to non-adiabatic case for any cyclic evolution of the quantum system itself, known as the Aharonov–Anandan (AA) phase,[3] which tends to the Berry phase in the adiabatic limit. Samuel and Bhandari generalized the Berry phase to non-cyclic and non-unitary cases.[7] Further generalizations have been studied in various physical systems like nonlinear systems,[14] mixed states,[15] and open systems.[16] Due to the geometric phases depend only on some global geometric features and show the robustness against certain noise,[17–19] they are potential for quantum computation and quantum information processing, and have been observed in various quantum systems.[6,9,11,21–25]

Comparing with the adiabatic geometric phase, which is constrained by the adiabatic condition in the actual experiments, leading to an intrinsic limitation on the operation time, the alternative nonadiabatic geometric phase is independent of the operation time, and then is more experimentally feasible.[26] However, because the quantum system with a true time-dependent Hamiltonian ordinarily is hard to solve analytically,[27] one has often to search for the various appropriate approximations to obtain the geometric phase. Recently, Landau–Zener–Stückelberg–Majorana (LZSM) interferometry has become a useful tool to handle a kind of time-dependent two-level system involved in geometric phase.[20,28–33] Based on the so-called adiabatic impulse model (AIM), one can obtain analytically the evolution of the state vector. Under the LZSM destructive interference condition, the system returns to the initial state after a cyclic evolution and the non-adiabatic geometric phase can be obtained related to the so-called Stokes phase.[28,31] However, the relation between both the destructive interference condition and the nonadibatic geometric phase with the system parameters is less obvious and not so direct to obtain. One may need a detailed description of how to manipulate the system to generate definite nonadiabatic geometric phases, which is help for quantum computation, for instance, building a universal quantum gate.[26,34,35]

In this work, we consider a doubly driven two-level system in which the two driving modes of Hamiltonian be adjusted by an additional relative phase. This model has recently been realized experimentally in an optical lattice clock (OLC) system, and observed clearly the interference between different Floquet channels by fine-tuning this relative phase.[36] Different from the previous work,[36] which was based on the resolved Floquet sideband approximation (RFSA) in the parameter region $g \ll \omega_s$, here we enter into the parameter regions $g > \omega_s$ that beyond the RFSA. With the help of AIM, we show various cases of the time evolution of system due to turn-on and -off of the gaps between energies controlled by the relative phase. The analytical results well agree with the

†Corresponding author. E-mail: tauwaang@cqu.edu.cn

© 2023 Chinese Physical Society and IOP Publishing Ltd

numerical results from numerical Floquet approach.[37,38] In addition, under the LZSM destructive interference condition, we show that the geometric phase (AA phase) accompanying a cyclic state evolution is related to the Stokes phase as well as the relative phase, and can be manipulated flexibly by the system parameters. Due to the signs of gaps of the eigenenergies changed by controlling the relative phase in the avoided crossing points, the geometric phase after a cyclic evolution characterizes two distinct phases in the adiabatic limit.

2. The model

We consider a doubly driven two-level system which is governed by the time-dependent Hamiltonian ($\hbar = 1$)

$$\hat{H}(t) = \frac{\varepsilon(t)}{2}\hat{\sigma}_z + \frac{\Delta(t)}{2}\hat{\sigma}_x, \tag{1}$$

with $\varepsilon(t) = \delta + A\omega_s\cos(\omega_s t)$ and $\Delta(t) = g\cos(\omega_s t + \psi)$ are respectively the longitudinal and transverse driving fields, where δ is a static bias, ω_s is the driving frequency, A and g are the longitudinal and transverse driving amplitudes, respectively, and ψ is the initial phase of the transverse driving field. $\hat{\sigma}_{x,z}$ are the Pauli matrices. Denote $|e\rangle$ and $|g\rangle$ as the eigenstates of $\hat{\sigma}_z$ with the corresponding eigenvalues ± 1, which are also the eigenstates of Hamiltonian (1) without the transverse drive [i.e., $\Delta(t) = 0$], forming the diabatic basis. When $A\omega_s > \delta$, the eigenenergies of Hamiltonian (1) without the transverse drive experience crossings at $t_{1,2} + nT$, where $\omega_s t_1 = \arccos(-\frac{\delta}{A\omega_s})$, $\omega_s t_2 = 2\pi - \omega_s t_1$, $n \in \mathbb{Z}$ and $T = 2\pi/\omega_s$. While due to the transverse coupling $\Delta(t)$, the instantaneous eigenenergies $E_\pm(t)$ of the Hamiltonian: $\hat{H}(t)\varphi_\pm(t) = E_\pm(t)\varphi_\pm(t)$, can exhibit the avoided crossing structures, where $E_\pm(t) = \pm\frac{1}{2}\Omega(t)$ with $\Omega(t) = \sqrt{\varepsilon^2(t) + \Delta^2(t)}$, and $\varphi_\pm(t) = \beta_\pm(t)|e\rangle \pm \beta_\mp(t)|g\rangle$ are the corresponding adiabatic instantaneous eigenstates with $\beta_\pm(t) = \sqrt{\frac{\Omega(t)\pm\varepsilon(t)}{2\Omega(t)}}$. When far away form the avoided crossings [$|\varepsilon(t)| \gg |\Delta(t)|$], the adiabatic eigenstates coincide with the diabatic basis.

We now study the time evolution of the system using AIM.[31,39] In this model, the system can be treated as experiencing the non-adiabatic transition just at the avoiding crossing point, apart from which the system undergoes a free adiabatic time evolution. The adiabatic evolution process is straightforward with the quantum adiabatic theory, whereas the non-adiabatic evolution is generally not easy to handle. But considering the non-adiabatic region is small enough and approximating the diabatic energies crossing as linearity near the crossing point, the evolution of system can be exactly obtained by solving the so-called Landau–Zener (LZ) problem.[40–43] Then the system evolution at the avoided crossing point can be described with a unitary evolution matrix (LZ transition matrix), concrete form of which depends on the approximate linearized LZ Hamiltonian in the vicinity of avoiding crossing point. To be specific, for the Hamiltonian given in Eq. (1), the diabatic energy crossing can be linearized in the vicinity of $t_{1,2}$, that is,

$$\mathrm{Re}\,\delta + A\omega_s\cos[\omega_s(t_{1,2} + t)] \approx \mp vt, \tag{2}$$

where $v = A\omega_s^2\sqrt{1 - \left(\frac{\delta}{A\omega_s}\right)^2}$. Then the Hamiltonian (1) can be approximately expressed by a linear LZ Hamiltonian in the vicinity of $t_{1,2}$

$$\hat{H}_{1,2} = \mp\frac{vt}{2}\hat{\sigma}_z + \frac{g_{1,2}}{2}\hat{\sigma}_x, \tag{3}$$

where $g_1 = g\cos[\arccos(-\frac{\delta}{A\omega_s}) + \psi]$, and $g_2 = g\cos[\arccos(-\frac{\delta}{A\omega_s}) - \psi]$. The minus (plus) sign in front of the first term in Eq. (3) applies to t_1 (t_2). When we describe the evolution of system in the diabatic basis, the LZ transition matrix depends both on the sign of diagonal and off-diagonal matrix element of the LZ Hamiltonian. So for the LZ Hamiltonian given in Eq. (3), the LZ transition matrix at t_1 and t_2 can be expressed respectively by[31]

$$X_1 = \begin{pmatrix} \sqrt{P_{\mathrm{LZ},1}} & -g_1'\sqrt{1 - P_{\mathrm{LZ},1}}\,\mathrm{e}^{\mathrm{i}\varphi_1} \\ g_1'\sqrt{1 - P_{\mathrm{LZ},1}}\,\mathrm{e}^{-\mathrm{i}\varphi_1} & \sqrt{P_{\mathrm{LZ},1}} \end{pmatrix}, \tag{4}$$

$$X_2 = \begin{pmatrix} \sqrt{P_{\mathrm{LZ},2}} & g_2'\sqrt{1 - P_{\mathrm{LZ},2}}\,\mathrm{e}^{-\mathrm{i}\varphi_2} \\ -g_2'\sqrt{1 - P_{\mathrm{LZ},2}}\,\mathrm{e}^{\mathrm{i}\varphi_2} & \sqrt{P_{\mathrm{LZ},2}} \end{pmatrix}, \tag{5}$$

where $P_{\mathrm{LZ},1(2)} = \exp[-2\pi\chi_{1(2)}]$ is the so-called LZ formula for the non-adiabatic transition,[40–43] $g_{1(2)}' = \mathrm{sgn}[g_{1(2)}]$, $\chi_{1(2)} = g_{1(2)}^2/(4v)$, and $\varphi_{1(2)} = \pi/4 + \chi_{1(2)}[\ln\chi_{1(2)} - 1] + \arg[\Gamma(1 - \mathrm{i}\chi_{1(2)})]$ is the Stokes phase. Note that the system may undergo different LZ transition probabilities P_{LZ} in t_1 and t_2 due to the phase ψ. In the slow-passage limit [$\chi_{1(2)} \gg 1$], which means the system will follow the adiabatic eigenstates, then $P_{\mathrm{LZ},1(2)} \approx 0$ and $\varphi_{1(2)} \approx 0$; by contrast, in the fast-passage limit [$\chi_{1(2)} \ll 1$], the system follows the diabatic states more probably, then we have $P_{\mathrm{LZ},1(2)} \approx 1$ and $\varphi_{1(2)} \approx \pi/4$.[31]

Between these avoided crossings, the system undergoes a free adiabatic evolution, which just accumulates a phase in the eigenstates. The adiabatic evolution can be described with the unitary matrix in the diabatic basis

$$U_\phi = \mathrm{e}^{-\mathrm{i}\phi\hat{\sigma}_z}, \tag{6}$$

where

$$\phi(t_f, t_i) = \frac{1}{2}\int_{t_i}^{t_f}\Omega(t)\,\mathrm{d}t. \tag{7}$$

Due to the diabatic energies crossing at t_1 and t_2, we find the unitary matrix Eq. (6) is suitable for evolution from $t_i = 0 + nT$ to $t_f = t_1 + nT$ and from $t_i = t_2 + nT$ to $t_f = t_1 + (n+1)T$, while the unitary matrix for evolution from $t_i = t_1 + nT$ to $t_f = t_2 + nT$ is given by U_ϕ^*, where $*$ indicates the complex conjugate. Then the system time evolution for the whole one-period can be described by the following combined unitary matrix:

$$U_T = U_{\phi_3}X_2U_{\phi_2}^*X_1U_{\phi_1} = \begin{pmatrix} \alpha & -\beta^* \\ \beta & \alpha^* \end{pmatrix}, \tag{8}$$

where

$$\alpha = g_1' g_2' \sqrt{(1-P_{\mathrm{LZ},1})(1-P_{\mathrm{LZ},2})}\, \mathrm{e}^{-\mathrm{i}\zeta_+} + \sqrt{P_{\mathrm{LZ},1}P_{\mathrm{LZ},2}}\, \mathrm{e}^{-\mathrm{i}\zeta_-}, \tag{9}$$

$$\beta = g_1' \sqrt{P_{\mathrm{LZ},2}(1-P_{\mathrm{LZ},1})}\, \mathrm{e}^{-\mathrm{i}(\phi_1+\phi_2-\phi_3+\varphi_1)} - g_2' \sqrt{P_{\mathrm{LZ},1}(1-P_{\mathrm{LZ},2})}\, \mathrm{e}^{\mathrm{i}(\phi_2+\phi_3-\phi_1+\varphi_2)}, \tag{10}$$

with $\zeta_+ = (\phi_1+\phi_3)+\phi_2+\varphi_1+\varphi_2$, $\zeta_- = (\phi_1+\phi_3)-\phi_2$, and $\phi_i = \phi(t_i, t_{i-1})$ with $t_3 = t_0 + T$. So an initial state $|\psi(t_0)\rangle = a_e|e\rangle + a_g|g\rangle$ will evolve to the final state after one single period as

$$\begin{aligned} |\psi(t_0+T)\rangle &= U_T|\psi(t_0)\rangle \\ &= (\alpha a_e - \beta^* a_g)|e\rangle + (\beta a_e + \alpha^* a_g)|g\rangle. \end{aligned} \tag{11}$$

If assuming the system is initially prepared in the ground state $|g\rangle$ at $t_0 = 0$, that is, $a_e = 0$ and $a_g = 1$ in Eq. (11), then the population probability of the excited state $|e\rangle$ after one single period can be calculated by

$$\begin{aligned} P_T &= |\beta|^2 \\ &= P_{\mathrm{LZ},1}(1-P_{\mathrm{LZ},2}) + P_{\mathrm{LZ},2}(1-P_{\mathrm{LZ},1}) \\ &\quad - 2g_1' g_2' \sqrt{P_{\mathrm{LZ},1}P_{\mathrm{LZ},2}(1-P_{\mathrm{LZ},1})(1-P_{\mathrm{LZ},2})} \\ &\quad \times \cos(\varphi_1+\varphi_2+2\phi_2). \end{aligned} \tag{12}$$

We can see the excited state population oscillates as a function of the interference phase $\phi_T = \varphi_1+\varphi_2+2\phi_2$, which is the so-called Stückelberg oscillation.[31,42] It can be interpreted as a quantum interference between the two different evolution paths of the system when passing successively two avoiding crossing points like an optical Mach–Zehnder interferometer. The maximum (minimum) of P_T correspond to the constructive (destructive) interference, which also relates to the sign of both g_1 and g_2 due to the relative phase ψ.

In the following we show some interesting results due to this relative phase ψ. We here just consider ψ ranging from 0 to π by noticing Eq. (12) are the same for ψ and $\psi+\pi$. This is because when replacing ψ with $\psi+\pi$, $g_{1,2}$ is just simultaneously replaced by $-g_{1,2}$, then the absolute values of α and β in Eqs. (9) and (10) keep unchanged, which leads to the same result Eq. (12).

At first, when $\delta = 0$, we have $g_1 = -g\sin\psi$ and $g_2 = g\sin\psi$. Then in the case of $\psi = 0$ and π, both g_1 and g_2 are equal to zero, which induces the avoided crossing to a real crossing,[44] and leads to a degeneracy of the adiabatic eigenenergies at the time instant $t_{1,2}+nT$ shown in the inset of Fig. 1.

Strictly speaking, both the diabatic and adiabatic energies exhibit crossings does not belong to the conventional LZ problem and the LZ formula is thus not applicable. In this case, one should search for other methods to study the time evolution of the system, i.e., need to analyze carefully the adiabatic evolution in this special case with the existence of a real degeneracy.[44,45] However, with the AIM, we can still consider the adiabatic evolution works everywhere except the real crossing points. Then the non-adiabatic transition probability at the crossing can be treated as an asymptotic value of the LZ formula as χ approaching zero. So for $g_1 = g_2 = 0$, we have $P_{\mathrm{LZ},1} = P_{\mathrm{LZ},2} \equiv 1$ and as a consequence $P_e = 0$, which implies that the system still keeps in the initial state $|g\rangle$ when crossing t_1 and t_2 as shown in Fig. 1(a). This is also similar to the results shown in Figs. 3(a) and 3(d) of Ref. [36], in which the effective Rabi frequency of zeroth sideband is zero for $\psi = 0$ or π. However, when A is comparable to g, the discrepancy between the diabatic and adiabatic states will induce the quantum transition to excited state even with a real crossing, then the AIM fails, as shown in Fig. 1(b). Another case is that $\psi \neq 0$ or π, the magnitude of both g_1 and g_2 can be controlled by the relative phase ψ. Then we can adjust only this phase to manipulate smoothly the system evolution from fast ($P_{\mathrm{LZ}} \simeq 1$) to slow ($P_{\mathrm{LZ}} \simeq 0$) limit or vice versa as shown in Fig. 2.

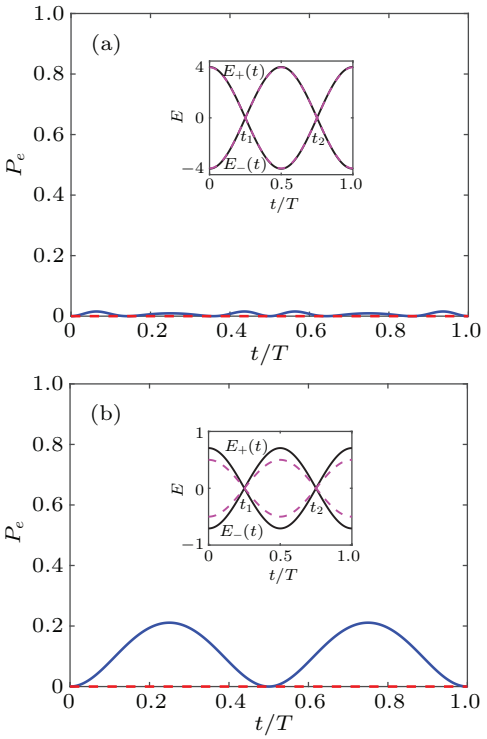


Fig. 1. The population probability of state $|e\rangle$ is plotted as a function of time with $\delta = 0$, $g/\omega_s = 1$, $\psi = 0$, (a) $A = 8$, and (b) $A = 1$. The solid blue lines are the numerical results from the Floquet method, and the dashed red lines are the theoretical results from AIM. The insets present the time evolution of energy levels during one period. Solid black lines and dashed magenta lines indicate the adiabatic and diabatic energy levels, respectively. There exists discrepancy in (b) between the results from AIM and the numerical Floquet method with small A.

When $\delta \neq 0$, both g_1 and g_2 are relevant to ψ. In this case, we can adjust the phase ψ to selectively turn on and off the gap at t_1 or t_2 independently, which also induce the avoided crossing to a real crossing. Closing up whichever the gap g_1 and

g_2 will lead to the interference disappearing, due to the system evolution becoming certain at the crossing and the resultant evolution path is definite. As shown in Fig. 3, the real crossing at t_1 (t_2) leads to the excitation probability just depends on $P_{\mathrm{LZ},2}$ ($P_{\mathrm{LZ},1}$) after one single period, which is irrelevant to the interference phase ϕ_T.

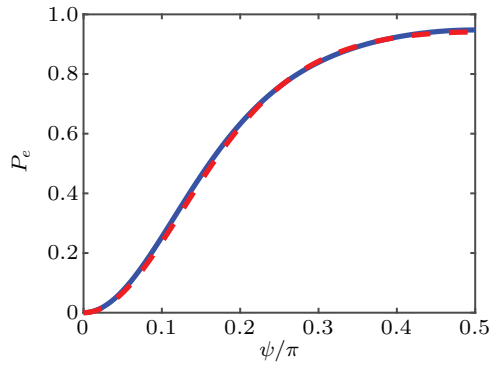


Fig. 2. The population probability of state $|e\rangle$ is plotted as a function of ψ at $t = T/2$ with $\delta = 0$, $A = 20$, $g/\omega_s = 6$. The solid blue line is the numerical result from the Floquet method, and the dashed red line is the theoretical result $1 - P_{\mathrm{LZ},1}$ from AIM.

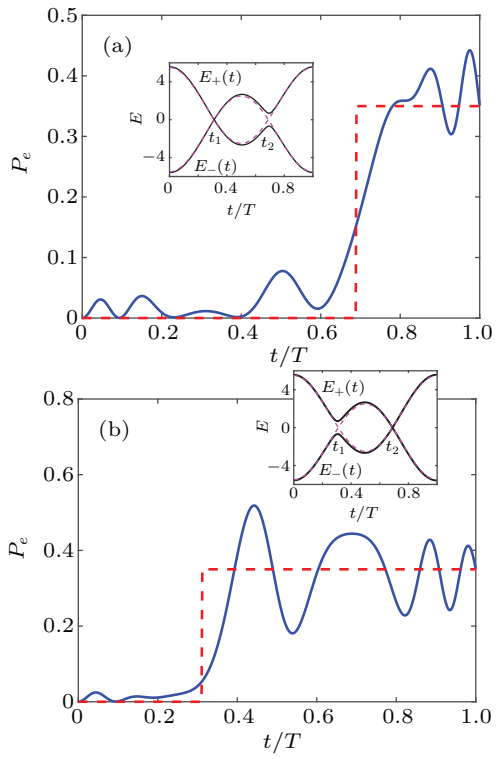


Fig. 3. The population probability of state $|e\rangle$ is plotted as a function of time with $\delta = 3$, $A = 8$, $g/\omega_s = 2$, (a) $\psi = 2.76$ and (b) $\psi = 0.38$. The solid blue lines are the numerical results from the Floquet method, and the dashed red lines are the theoretical results from AIM. The insets present the time evolution of energy levels during one period. Solid black lines and dashed magenta lines indicate the adiabatic and diabatic energy levels, respectively.

3. Geometric phase accompanying cyclic state evolution

When a physical system undergoes a cyclic evolution and returns to its initial state, the geometric phase can be defined by removing the dynamic phase from the total phase.[3] With the AIM and given the initial state $|\psi(t_0 = 0)\rangle = |g\rangle$, the condition for system returning to the initial state after one single period is given by $\beta = 0$ and the resultant finial state can be expressed from Eq. (11) by $|\psi(T)\rangle = \exp(\mathrm{i}\Phi)|g\rangle$ with $\Phi = -\arg(\alpha)$ as the total phase. In addition, the dynamical phase can be expressed as[3,28]

$$\begin{aligned}\gamma_{\mathrm{d}} &= -\int_0^T \langle\psi(t)|\hat{H}(t)|\psi(t)\rangle\,\mathrm{d}t \\ &= \phi_1 + \phi_3 + (1 - 2P_{\mathrm{LZ},1})\phi_2. \end{aligned} \tag{13}$$

Therefore, the geometric phase can be obtained by

$$\gamma_{\mathrm{g}} = \Phi - (\phi_1 + \phi_3) - (1 - 2P_{\mathrm{LZ},1})\phi_2. \tag{14}$$

In the following, we consider mainly two cases in which the geometric phase emerging with different conditions and can characterize two distinct phases in the adiabatic limit.

Case (i) We consider firstly the case of $\delta = 0$. We have $P_{\mathrm{LZ},1} = P_{\mathrm{LZ},2}$, $\varphi_1 = \varphi_2$, $\phi_1 + \phi_3 = \phi_2$, and $g_1' = -g_2'$. Thus the single-period transition probability Eq. (12) is reduced to $P_T = 4P_{\mathrm{LZ},1}(1 - P_{\mathrm{LZ},1})\cos^2(\varphi_1 + \phi_2)$, so the condition for system returning to its initial state is given by

$$\varphi_1 + \phi_2 = (1/2 + n)\pi. \tag{15}$$

We show the interference phase ϕ_T changing with A and ϕ in Fig. 4. And one can always manipulate A and ψ to make the system return to initial state with the condition Eq. (15), which corresponds to the dashed red lines in Fig. 4.

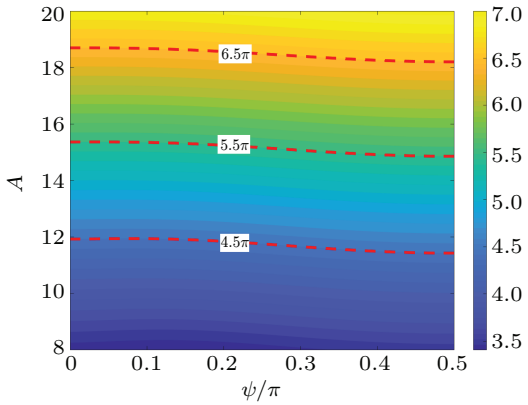


Fig. 4. The interference phase ϕ_T is plotted as a function of A and ψ with $\delta = 0$, $g/\omega_s = 6$. The dashed red lines form up to bottom indicate the destructive interference with $\phi_T = 6.5\pi$, 5.5π, 4.5π, respectively.

Then the final state becomes $|\psi(T)\rangle = |g\rangle$ with the total phase $\Phi = 0$, which means the dynamical phase is totally compensated by the geometric phase, thus the geometric phase can be obtained by

$$\gamma_{\mathrm{g}} = -2\phi_2(1 - P_{\mathrm{LZ},1}) \mod(2\pi). \tag{16}$$

We can see the geometric phase is related to the Stokes phase as well as the relative phase ψ. In the adiabatic limit, we have $P_{\mathrm{LZ},1(2)} \simeq 0$ and $\varphi_{1(2)} \simeq 0$, then the geometric phase Eq. (16)

under the condition Eq. (15) is reduced to the adiabatic Berry phase $\chi_g \simeq -\phi_2 = -\pi$ [mod(2π)]. In Fig. 5, we show an example for the geometric phase changing with ψ under the condition $\phi_T = 4.5\pi$ (the bottom dashed red line in Fig. 4). And it is shown that the geometric phase approaches $-\pi$ in the adiabatic limit ($P_{\mathrm{LZ},1}$ tends to 0 shown in the inset).

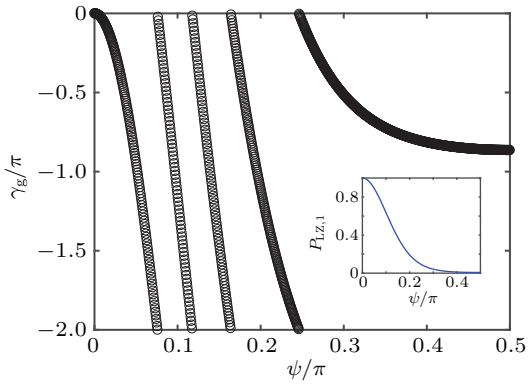


Fig. 5. Geometric phase Eq. (19) as a function of ψ with $\delta = 0$, $g/\omega_s = 6$ under the condition $\psi_T = 4.5\pi$. The inset shows the LZ transition probability changing with ψ under the same condition.

Case (ii) We consider $\delta \neq 0$ and $\psi = 0$. We have $P_{\mathrm{LZ},1} = P_{\mathrm{LZ},2}$, $\varphi_1 = \varphi_2$, and $g_1 = g_2$. Then the single-period transition probability Eq. (12) is reduced to $P_T = 4P_{\mathrm{LZ},1}(1 - P_{\mathrm{LZ},1})\sin^2(\varphi_1 + \phi_2)$, so the condition for system returning to its initial state is given by

$$\varphi_1 + \phi_2 = n\pi. \tag{17}$$

We also show the interference phase ϕ_T changing with A and δ in Fig. 6. The dashed red lines indicate the condition Eq. (17) for the system returning to the initial state.

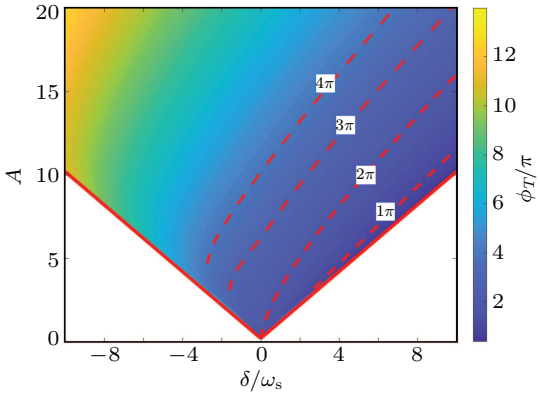


Fig. 6. The interference phase ϕ_T is plotted as a function of A and δ with $g/\omega_s = 6$, $\psi = 0$. The dashed red lines form up to bottom indicate the destructive interference with $\phi_T = 4\pi$, 3π, 2π, and 1π, respectively. The inclined red lines show the region of the validity of the LZSM theory: the region above lines indicates the system can experience avoiding crossing.

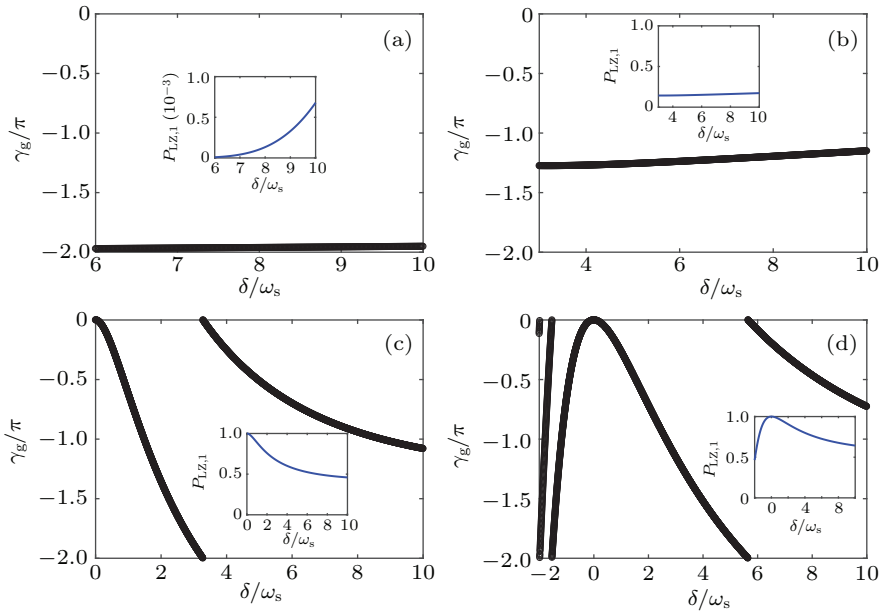


Fig. 7. Geometric phase Eq. (18) as a function of ψ with $g/\omega_s = 6$, $\psi = 0$ under the condition $A > g$ and (a) $\psi_T = 1\pi$, (b) $\psi_T = 2\pi$, (c) $\psi_T = 3\pi$, and (d) $\psi_T = 4\pi$, respectively. The inset shows the LZ transition probability changing with ψ under the same condition.

Under this condition, the final state is $|\psi(T)\rangle = \mathrm{e}^{\mathrm{i}\zeta_-}|g\rangle$ with the total phase $\Phi = \zeta_-$. Thus the geometric phase can be obtained by

$$\begin{aligned}\gamma_g &= \zeta_- - (\phi_1 + \phi_3) - (1 - 2P_{\mathrm{LZ},1})\phi_2 \\ &= -2\phi_2(1 - P_{\mathrm{LZ},1}) \mod(2\pi),\end{aligned} \tag{18}$$

which holds the same form with the case of $\delta = 0$. In the adiabatic limit, however, the geometric phase approaches 0 instead of $-\pi$. In Fig. 7, we show the geometric phase changing with δ under different destructive interference conditions. And it is shown that the adiabatic geometric phase approaches 0 (-2π) as shown in Fig. 7(a).

On the other hand, the nonadiabatic geometric phase for the two-level system can be more clearly visualized by a circuit C in the projective Hilbert space.[3,6] We can map the state evolution $|\psi(t)\rangle$ into a unit vector $\boldsymbol{n} =$

$(\sin\Theta\cos\Phi, \sin\Theta\sin\Phi, \cos\Theta)$ on the Bloch sphere spanned by the diabatic basis via the relation $\boldsymbol{n}(t) = \langle\psi(t)|\boldsymbol{\sigma}|\psi(t)\rangle$. Then the geometric phase is related to the solid angle subtended by the evolution circuit C on the Bloch sphere as

$$\gamma_{\rm g} = -\frac{1}{2}\Omega(C). \tag{19}$$

In the frame of AIM, the state evolution is obtained with the combined unitary evolution matrix Eq. (8) with the initial state $|\psi(0)\rangle = |g\rangle$. Thus, the evolution circuit can be described as follows. In the stage $t = 0$ to $t = t_1$, the state remains at the south pole; at the time $t = t_1$, the vector suddenly moves along a meridian to the point (Θ_1, Φ_1) (here Θ is the angle between the vector and south pole) via the fist LZ transition, where $\Theta_1 = 2\arccos\sqrt{P_{\rm LZ,1}}$ and $\Phi_1 = \varphi_1 + (1+g_1')\pi/2$; in the second stage, the vector moves along the parallel to (Θ_1, Φ_2), where $\Phi_2 = \Phi_1 + 2\phi_2$; at the time $t = t_2$, the system undergoes the second LZ transition. For both the two cases discussed above, it suddenly moves back to the south pole and then stays there until $t = T$. The solid angle subtended by this cyclic curve C is $\Omega(C) = 4\phi_2(1 - P_{\rm LZ,1})$. Then the geometric phase $\gamma_{\rm g} = -2\phi_2(1 - P_{\rm LZ,1})$, which is identical to Eqs. (16) and (18). In the adiabatic limit, the two cases show distinct vector traveling paths on the sphere: for case (i), the vector first moves along the meridian from south pole to north with $\Phi_1 = 0$, and then back to south with $\Phi_2 = \pi$ [due to $2\phi_2 = \pi{\rm mod}(2\pi)$], thus the vector travels on the sphere forms a great circle that makes $\gamma_{\rm g} = -\pi$; for case (ii), the vector moves along the meridian from south pole to north with $\Phi_1 = 0$ but back to south along the original path (due to $\phi_2 = n\pi$), which makes the geometric phase $\gamma_{\rm g} = 0$.

4. Discussion and conclusion

In this work, we study a time-periodic driven two-level system, of which the Hamiltonian are both in longitudinal and transverse modulation. Due to the on-off of gaps of the system eigenenergies being controlled by the relative phase of the driving modes, the time evolution of the system is strongly related to this phase. In the parameter region with large longitudinal driving amplitude, with the help of AIM, we show that when both the two gaps in one driving period closed, the system will be trapped in the initial state, but the noncoincidence between the adiabatic and diabatic states induced by small driving amplitude will lead to the discrepancy between the AIM results and accurate numerical results; when just one of the two gaps closed, the interference effect will disappear and the tunneling probability to the excited state depends only on the LZ formula at another avoided crossing. These analytic results are confirmed with the help of numerical Floquet method. In addition, we determine the non-adiabatic geometric phase accompanying a cyclic evolution under the condition of destructive LZSM interference, and show that it can be manipulated by the relative phase. In the adiabatic limit, this geometric phase tends to $-\pi$ for $\delta = 0$ and 0 for $\delta \neq 0$, $\psi = 0$, respectively.

The time evolution processes and the nonadiabatic geometric phase in our model with a true time-dependent Hamiltonian can possibly be measured experimentally in the OLC system.[36,46–48] The parameters region $g > \omega_{\rm s}$ which beyond the previous work[36] can be touched by increasing the intensity of the clock laser or decreasing the driving frequency.[46] It is worth noting that the dephasing effect due to temperature must be handled appropriately in the real OLC system.[46] However, we can utilize the spin-echo technique to remove the dynamic phase, making the state evolution purely geometric dependent and then resilient to dephasing effect.[26,34] In conclusion, the results discussed in this work pave the way for observing and manipulating the nonadiabatic geometric phase in the OLC system.

Acknowledgements

Project supported by the Special Foundation for theoretical physics Research Program of China (Grant No. 11647165) and the China Postdoctoral Science Foundation Funded Project (Project No. 2020M673118). W.-D.L. acknowledges the funding from the National Natural Science Foundation of China (Grant No. 11874247), the National Key Research and Development Program of China (Grant No. 2017YFA0304500), the Program of State Key Laboratory of Quantum Optics and Quantum Optics Devices, China (Grant No. KF201703), and the support from Guangdong Provincial Key Laboratory (Grant No. 2019B121203002).

References

[1] Berry M V 1984 *Proc. R. Soc. London, Ser. A* **392** 54
[2] Wilczek F and Zee A 1984 *Phys. Rev. Lett.* **52** 2111
[3] Aharonov Y and Anandan J 1987 *Phys. Rev. Lett.* **58** 1593
[4] Shapere A and Wilczek F 1989 *Geometric Phases in Physics* (Singapore: World Scientific)
[5] Simon B 1983 *Phys. Rev. Lett.* **51** 2167
[6] Suter D, Mueller K T and Pines A 1988 *Phys. Rev. Lett.* **60** 1218
[7] Samuel J and Bhandari R 1988 *Phys. Rev. Lett.* **60** 2339
[8] Mead C A 1992 *Rev. Mod. Phys.* **64** 51
[9] Zhang Y B, Tan Y W, Stormer H L and Kim P 2005 *Nature* **438** 201
[10] Tong D M, Singh K, Kwek L C, Fan X J and Oh C H 2005 *Phys. Lett. A* **339** 288
[11] Leek P J, Fink J M, Blais A, Bianchetti R, Göppl M, Gambetta J M, Schuster D I, Frunzio L, Schoelkopf R J and Wallraff A 2007 *Science* **318** 1889
[12] Xiao D, Chang M C and Niu Q 2010 *Rev. Mod. Phys.* **82** 1959
[13] Abdel-Khalek S, Berrada K, Mohamed A E S and Abel-Aty M 2013 *Chin. Phys. B* **22** 100301
[14] Wu B, Liu J and Niu Q 2005 *Phys. Rev. Lett.* **94** 140402
[15] Sjöqvist E, Pati A K, Ekert A, Anandan J S, Ericsson M, Oi D K L and Vedral V 2000 *Phys. Rev. Lett.* **85** 2845
[16] Carollo A, Fuentes-Guridi I, Santos M F and Vedral V 2003 *Phys. Rev. Lett.* **90** 160402
[17] de Chiara G and Palma G M 2003 *Phys. Rev. Lett.* **91** 090404

[18] Zhu S L and Zanardi P 2005 *Phys. Rev. A* **72** 020301
[19] Filipp S, Klepp J, Hasegawa Y, Plonka-Spehr C, Schmidt U, Geltenbort P and Rauch H 2009 *Phys. Rev. Lett.* **102** 030404
[20] Tan X, Zhang D W, Zhang Z, Yu Y, Han S and Zhu S L 2014 *Phys. Rev. Lett.* **112** 027001
[21] Möttönen M, Vartiainen J J and Pekola J P 2008 *Phys. Rev. Lett.* **100** 177201
[22] Webb C L, Godun R M, Summy G S, Oberthaler M K, Featonby P D, Foot C J and Burnett K 1999 *Phys. Rev. A* **60** R1783
[23] Atala M, Aidelsburger M, Barreiro J T, Abanin D, Kitagawa T, Demler E and Bloch I 2013 *Nat. Phys.* **9** 795
[24] Abdumalikov Jr A A, Fink J M, Juliusson K, Pechal M, Berger S, Wallraff A and Filipp S 2013 *Nature* **496** 482
[25] Zhang L B, Song C, Wang H H and Zheng S B 2018 *Chin. Phys. B* **27** 070303
[26] Zhu S L and Wang Z D 2002 *Phys. Rev. Lett.* **89** 097902
[27] Barnes E and Das Sarma S 2012 *Phys. Rev. Lett.* **109** 060401
[28] Kayanuma Y 1997 *Phys. Rev. A* **55** R2495
[29] Gasparinetti S, Solinas P and Pekola J P 2011 *Phys. Rev. Lett.* **107** 207002
[30] Zhang J, Zhang J, Zhang X and Kim K 2014 *Phys. Rev. A* **89** 013608
[31] Shevchenko S, Ashhab S and Nori F 2010 *Phys. Rep.* **492** 1
[32] Wang L, Tu T, Gong B, Zhou C and Guo G C 2016 *Sci. Rep.* **6** 19048
[33] Ivakhnenko O V, Shevchenko S N and Nori F 2022 ArXiv: 2203.16348 [quant-ph]
[34] Wang X B and Matsumoto K J 2001 *Phys. Rev. Lett.* **87** 097901
[35] Ji Y H, Cai S H, Le J X and Wang Z S 2010 *Chin. Phys. B* **19** 010311
[36] Lu X T, Wang T, Li T, Zhou C H, Yin M J, Wang Y B, Zhang X F and Chang H 2021 *Phys. Rev. Lett.* **127** 033601
[37] Shirley J H 1965 *Phys. Rev.* **138** B979
[38] Eckardt A 2017 *Rev. Mod. Phys.* **89** 011004
[39] Damski B and Zurek W H 2006 *Phys. Rev. A* **73** 063405
[40] Landau L D 1932 *Phys. Z. Sowjetunion* **2** 46
[41] Zener C 1932 *Proc. R. Soc. A* **137** 696
[42] Stückelberg E C G 1932 *Helv. Phys. Acta* **5** 369
[43] Majorana E 1932 *Nuovo Cimento* **9** 43
[44] Militello B D and Vitanov N V 2015 *Phys. Rev. A* **91** 053402
[45] Lehto J and Suominen K A 2012 *Phys. Rev. A* **86** 033415
[46] Liu W X, Wang T, Zhang X F and Li W D 2021 *Phys. Rev. A* **104** 053318
[47] Yin M J, Lu X T, Li T, Xia J J, Wang T, Zhang X F and Chang H 2022 *Phys. Rev. Lett.* **128** 073603
[48] Yin M J, Wang T, Lu X T, Li T, Wang Y B, Zhang X F, Li W D, Smerzi A and Chang H 2021 *Chin. Phys. Lett.* **38** 073201
[49] Sjöqvist E 2008 *Physics* **1** 35
[50] Sjöqvist E 2015 *Int. J. Quantum Chem.* **115** 1311